Statistical Analysis of Random Boundary Conditions in a Reverberation Chamber

(Article begins on next page)

Statistical Analysis of Random Boundary Conditions in a Reverberation Chamber

Jawad Ali
Dep. of Information Engineering
Università Politecnica delle Marche
Ancona, Italy
j.ali@univpm.it

Paola Tili
Dep. of Information Engineering
Università Politecnica delle Marche
Ancona, Italy

Luca Bastianelli
Dep. di Ingegneria Civile, Edile, Architettura
Università Politecnica delle Marche
Ancona, Italy

Alfredo de Leo
Dep. of Information Engineering
Università Politecnica delle Marche
Ancona, Italy

Valter Mariani Primiani
Dep. of Information Engineering
Università Politecnica delle Marche
Ancona, Italy

Franco Moglie
Dep. of Information Engineering
Università Politecnica delle Marche
Ancona, Italy

***Abstract*—In this paper, a comprehensive statistical analysis of the Reverberation Chamber with random boundaries and a mechanical stirrer is performed to evaluate the field correlation for independent positions achieved from a stirred electromagnetic field. The analysis of the reverberation chamber is conducted through numerical simulation by using a custom FDTD solver. The reverberant environment is modeled with two monopole antennas along with N_s 64 random boundaries and stirrer positions. The degree of independence among the field samples is quantified through the spatial correlation matrix, while the Kolmogorov–Smirnov (KS) statistics provides an additional measure of statistical consistency. The use of randomized boundaries enables a well-stirred field across the chamber, and even though a residual unstirred energy may occur at lower frequencies due to the limited number of resonant modes, proper matching of the chamber size to the working frequency ensures effective stirring. The addition of a mechanical stirrer further enhances field uniformity and increases the number of independent positions even for a small-volume Reverberation Chamber, providing insights for efficient chamber design and characterization.**

***Index Terms*—Reverberation Chamber, Random Boundaries, Spatial correlation Matrix, Field Uniformity, Kolmogorov–Smirnov statistics**

I. INTRODUCTION

The creation of a multi-path reflecting environment in a Reverberation Chamber (RC) for electromagnetic compatibility (EMC) testing is effective if we have a statistically uniform field with a high number of independent samples. The number of independent samples in the chamber depends on several factors, like the chamber dimensions [1], frequency [2] , and loading conditions [3] , but mostly on the stirring mechanism [4]. Different stirring mechanisms are used in the RC, like mechanical stirring (MS) [4], frequency stirring [5], and source stirring [6]. Based on this, the samples independence is measured by defining the correlation between the two field measurements at different stirrer positions, frequencies, or points in the working volume (WV). The statistical analysis of the field in the RC is mostly performed using the auto-correlation function (ACF) [7], cross-correlation function (CCF) [8], Kolmogorov–Smirnov (KS) goodness-of-fit test [9], Spatial or stirrer correlation matrix [10], or a hybrid approach [11]. Among these, ACF is the most prominent method that is used in most of the RC with regular boundaries [12]. This gives the correlation for adjacent and near-adjacent samples in the chaotic environment, giving N_{ind} the number of independent samples [13]. In case of Random boundaries (RB) used as a stirring mechanism [14] to produce a statistically uniform field inside the RC, ACF is not feasible due to its sequential uniformity check [15]. Instead, the statistical evaluation must rely on non-sequential techniques, such as ensemble-based methods or independent sample extraction, to ensure that each realization represents a distinct and uncorrelated field distribution. Similarly, the measurements are taken inside the WV, which is mostly uniform, but it is taken at a single point, and the ACF varies spatially in the WV [12]. When the test object or reference antenna is not electrically small, the spatial correlation of the fields becomes an important factor in understanding and predicting its measured response inside the chamber [16]. The statistical analysis of independent samples in an RC with RB conditions is performed using a correlation-based threshold, typically defined as $|\rho| < 0.37$ (IEC/CISPR criterion) or equivalently $\rho < 1/e$ [11]. A pairwise spatial correlation is executed at a single frequency between N_s RB/stirrer positions. This leads us to perform a numerical analysis of the uncorrelated positions, adopting a spatial correlation matrix in the WV in this paper. We adopt a statistical analysis approach rooted in the spatial correlation matrix to evaluate the effectiveness of RB stirring in the RC. Since RB configurations do not produce sequential field variations, traditional ACF-based methods cannot be applied; instead, the correlation of samples must be assessed through pairwise spatial correlations between field realizations.

This work is supported by MSCA TMA DN NEPIT - Network for Evaluation of Propagation and Interference Training. This project has received funding from the European Union's Horizon Europe - Research and Innovation program - under grant agreement no. 101119806.

This aligns directly with the ensemble-based interpretation, where uncorrelated samples correspond to low inter-sample correlation measured across different RB/stirrer positions.

II. Methodology

All simulations were carried out using a customized FDTD code developed by the EMC group at UNIVPM [17]. A structured sampling approach is implemented on the boundaries of the RC in the computational domain [14]. A set of points $P(i_x, i_y, i_z)$ on the chamber walls with a thickness of 50 cells is generated with a repetition after every 3 cells. If $B_o(\mathbf{r})$ denotes the baseline boundary condition, then for the k-th realization, we define the perturbed boundary as:

$$B_k(\mathbf{r}) = B_o(\mathbf{r}) + \Delta B_k(\mathbf{r}) \tag{1}$$

where $\Delta B_k(\mathbf{r})$ is a spatially localized random field with zero mean and bounded variance. The large scale generation of the perturbed points is memory efficient due to this structured approach. These RB, together with the MS, allow us to study how the field distribution inside the chamber changes from one configuration to another. The simulation environment is organized into three main parts: the FDTD, the FFT post-processing step, and the statistical module, where the spatial correlation matrix is computed for all the field coefficients. All three parts are parallelized to manage the large number of configurations required for the correlation-based analysis.

A. Simulation setup

The RB condition is generated using the method defined in our previous work [14], with a cell dimension of 3 mm. The geometry of the simulated RC is $542 \times 642 \times 722$ cells in the Cartesian plane. Fig. 1 illustrates the geometry of the proposed RC designed with RB conditions and a stirrer. The chamber contains two monopoles of the same size, 61 mm along the $+\hat{z}$ direction, with a MS and input of 64 changing RB/stirrer positions. The monopoles' position in the grid, in accordance with the cell location are:

- Monopole #1: 100 ($\hat{x}$), 140 ($\hat{y}$), 0 ($\hat{z}$);
- Monopole #2: 450 ($\hat{x}$), 550 ($\hat{y}$), 0 ($\hat{z}$);

A Gaussian pulse modulated sinusoid is used as an excitation signal for the band of interest. The frequency band taken is from 1.0 GHz to 10 GHz, and the separation between the RB, stirrer, and the monopoles is $\lambda/4$. A virtual volumetric loss $\sigma = 10^{-5}$ S/m is introduced to mimic the real losses in the chamber, which is useful to speed up the numerical simulations [17]. A 1.9 ps time step is taken per measurement in the time domain with the 3 mm cubic cells. Each simulation includes the full FDTD time-domain run, the FFT-based conversion to the frequency domain, and the subsequent statistical processing across the various RB/stirrer positions. When executed on CINECA's Leonardo high-performance computing (HPC) system, the entire workflow takes 9 hours of wall-clock time. The computations were carried out on 8 compute nodes using a parallelized MPI-based distributed memory configuration.

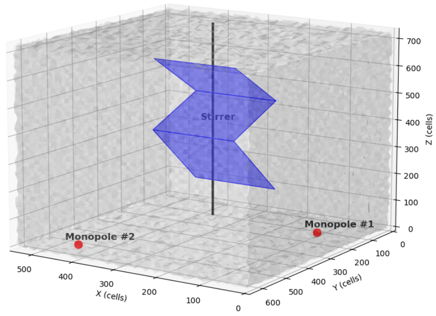

Fig. 1. Schematics of the geometry of the RC with RB and stirrer.

B. Spatial Correlation Analysis

The statistical analysis of the RC with RB is carried out using a spatial correlation matrix approach, which allows evaluating the independence of field realizations across the working volume. The field is sampled at N_s spatial points inside the chamber for each stirrer position. For the j-th stirrer position, the field values are arranged into a vector,

$$\mathbf{e}_j = [e_{j,1}, e_{j,2}, \ldots, e_{j,N_s}] \tag{2}$$

where $e_{j,i}$ represents the field at the i-th spatial point. The mean field vector over all RB/stirrer positions is calculated as,

$$\boldsymbol{\mu} = \frac{1}{N_s} \sum_{j=1}^{N_s} \mathbf{e}_{j,N_s} \tag{3}$$

capturing the average behavior of the chamber. Using these vectors, the correlation matrix $\mathbf{\Sigma}$ is computed as,

$$\mathbf{\Sigma} = \mathbb{E}\left[(\mathbf{e} - \boldsymbol{\mu})(\mathbf{e} - \boldsymbol{\mu})^T\right] \tag{4}$$

where $\mathbb{E}[\cdot]$ denotes the ensemble average over all stirrer positions. The diagonal elements of $\mathbf{\Sigma}$ correspond to the variance at the same spatial point, while the off-diagonal elements quantify the correlation between pairs of points. Large off-diagonal terms indicate strong correlations, implying that fewer independent field realizations are present.

$$\Sigma = \begin{bmatrix} \sigma_{11} & \sigma_{12} & \cdots & \sigma_{1N_s} \\ \sigma_{21} & \sigma_{22} & \cdots & \sigma_{2N_s} \\ \vdots & \vdots & \ddots & \vdots \\ \sigma_{N_s1} & \sigma_{N_s2} & \cdots & \sigma_{N_sN_s} \end{bmatrix}$$

To standardize the covariance values, the correlation matrix $\mathbf{R}$ is defined as,

$$\mathbf{R} = (\mathrm{Tr}(\mathbf{\Sigma}))^{-1/2}\, \mathbf{\Sigma}\, (\mathrm{Tr}(\mathbf{\Sigma}))^{-1/2} \tag{5}$$

where $\mathrm{Tr}(\mathbf{\Sigma})$ is the trace of the covariance matrix. Each element ρ_{jk} of $\mathbf{R}$ represents the Pearson correlation coefficient between two spatial points. Positions with $\rho_{jk} \approx 1$ are strongly correlated and do not contribute to independent sampling, while positions with $\rho_{jk} \approx 0$ are statistically independent. The number of independent samples, N_{ind}, is estimated by applying a correlation threshold, typically $|\rho| < 0.37$ (or equivalently $\rho < 1/e$), across the correlation matrix. Since some positions

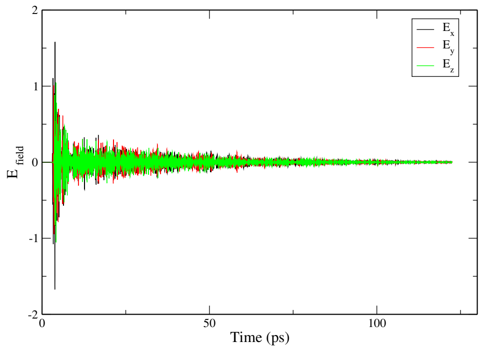

Fig. 2. Time-domain behavior of the three cartesian components of the electric field.

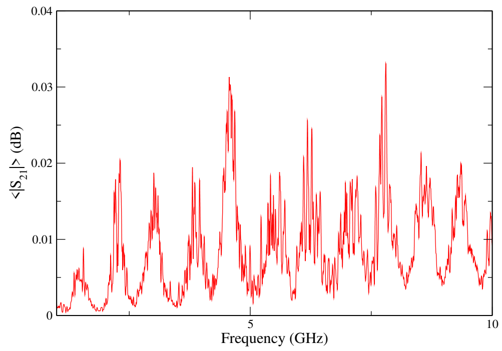

Fig. 3. Average of the transmission coefficient amplitude for the monopole.

are correlated, the total number of independent realizations is generally less than the number of RB/stirrer positions,

$$N_{\text{ind}} \leq N_s \tag{6}$$

III. Results

The results from the simulations using both RB conditions and mechanical stirring are presented with emphasis on spatial correlation analysis. The spatial correlation matrix is employed to quantify the independence of field samples and evaluate the effectiveness of the combined stirring mechanisms. The Electric field S_{21} and the unstirred energy measured show the chamber's characteristic behavior. To further examine performance and statistical consistency, the Kolmogorov–Smirnov (KS) statistic is applied. Together, these analyses provide a concise evaluation of the RC.

The time-domain decay of the electric field inside the chamber is shown in Fig. 2. The results indicate that the electromagnetic energy attenuates appropriately over time in the RC with RB. Fig. 3 presents the average complex transmission coefficient $< |S_{21}| >$ for N_s RB/stirrer positions. An estimate of the independent positions within the chamber is provided in Fig. 4. This is done using KS statistics with the acceptance threshold set, which shows the empirical distribution of the measured samples relative to the theoretical distribution in a fully stirred environment. The frequencies at which the KS statistics exceed the acceptance threshold point out to the positions that are considered statistically independent, indicating effective stirring and adequate field variability across those sample locations.

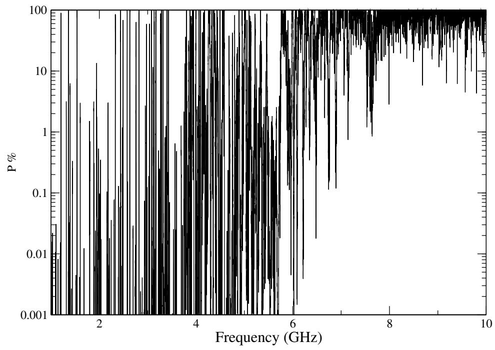

Fig. 4. KS statistics as a function of frequency for RB simulations

Fig. 5 illustrates the K-factor in the RC across the frequency range. As the K-factor shows the ratio between unstirred and stirred energy, we observe that in lower frequency range, the amount of unstirred energy is high due to the compact size of the RC.

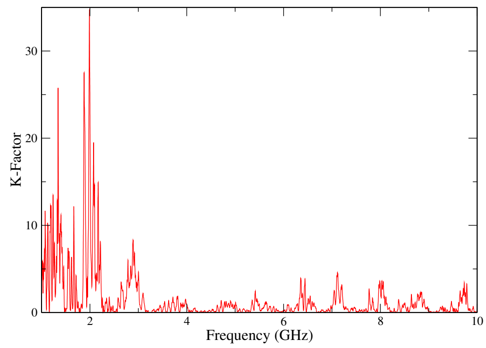

Fig. 5. K-factor analysis of the unstirred and stirred energy in the frequency range.

The spatial correlation analysis along the field components for the chamber with RB is presented in Fig. 6. It can be observed that the results are in good agreement with the chamber's unstirred energy. The number of independent positions, N_s, with respect to the random geometries is equal to $N_{ind} = 64$ at high frequency.

Similarly, an analysis of a hybrid approach combining RB with a MS is presented in Fig. 7. It can be observed that by using a hybrid stirring approach increases the number of independent positions at lower frequencies. This indicates that a chamber with a smaller geometry can achieve a more uniform and randomized field distribution when using a hybrid stirring technique.

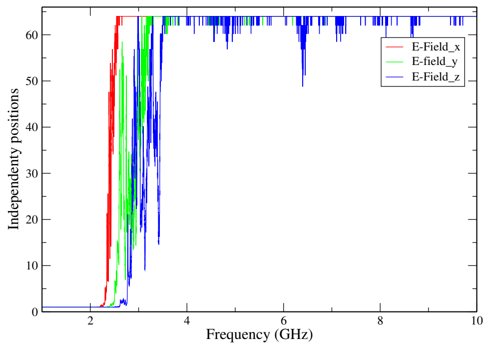

Fig. 6. Spatial correlation matrix based analysis for independent position with RB.

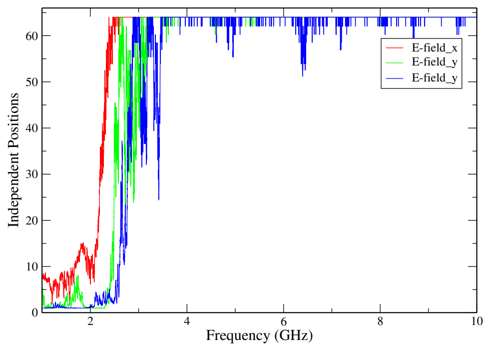

Fig. 7. Spatial correlation matrix based analysis for independent position with RB and MS.

IV. Conclusion

In this work, a numerical analysis of the RC with RB and a MSr is performed to compare the methods based on the number of independent samples in the chamber. The field uniformity and resonant fields within the RC are evaluated using the spatial correlation matrix approach, which effectively quantifies the field correlation within the working volume. The findings reveal that RB alone can produce statistically uniform fields. Furthermore, with a hybrid approach, a more randomized field can be achieved at lower frequencies in a small chamber by combining RB and a MS. The combination of RB and mechanical stirring techniques is shown to improve the number of independent samples and overall statistical performance, providing a reliable method for optimizing RC designs for electromagnetic compatibility testing. Future work will focus on the experimental validation of the RB approach to achieve a more precise and robust testing methodology in the RC. Another promising direction is the exploration of alternative boundary types, such as structured or semi-RB, to assess their impact on field uniformity, statistical de-correlation, and overall chamber performance.

Acknowledgment

We acknowledge EuroHPC Joint Undertaking for awarding us access to Leonardo at CINECA, Italy.

References

[1] F. Moglie and V. M. Primiani, "Numerical analysis of a new location for the working volume inside a reverberation chamber," *IEEE Transactions on Electromagnetic Compatibility*, vol. 54, no. 2, pp. 238–245, 2012.
[2] M. Hatfield and M. Slocum, "Frequency characterization of reverberation chambers," in *Proceedings of Symposium on Electromagnetic Compatibility*. IEEE, 1996, pp. 190–193.
[3] J. B. Coder, J. M. Ladbury, C. L. Holloway, and K. A. Remley, "Examining the true effectiveness of loading a reverberation chamber: How to get your chamber consistently loaded," in *2010 IEEE International Symposium on Electromagnetic Compatibility*. IEEE, 2010, pp. 530–535.
[4] C. F. Carobbi and R. Serra, "Analysis of concurrent and correlated stirring mechanisms in reverberation chambers," *IEEE Transactions on Electromagnetic Compatibility*, vol. 65, no. 3, pp. 607–616, 2023.
[5] U. Carlberg, P.-S. Kildal, and J. Carlsson, "Numerical study of position stirring and frequency stirring in a loaded reverberation chamber," *IEEE Transactions on Electromagnetic Compatibility*, vol. 51, no. 1, pp. 12–17, 2009.
[6] G. Cerri, V. M. Primiani, S. Pennesi, and P. Russo, "Source stirring mode for reverberation chambers," *IEEE transactions on electromagnetic compatibility*, vol. 47, no. 4, pp. 815–823, 2006.
[7] G. Gradoni, L. Bastianelli, V. M. Primiani, and F. Moglie, "Uncorrelated frequency steps in a reverberation chamber: A multivariate approach," in *2015 IEEE International Symposium on Electromagnetic Compatibility (EMC)*. IEEE, 2015, pp. 558–562.
[8] M. Tamart, F. Sarrazin, E. Richalot, M. Davy, and J. de Rosny, "Diffuse field cross-correlation in a reverberantion chamber," in *2020 IEEE International Symposium on Antennas and Propagation and North American Radio Science Meeting*. IEEE, 2020, pp. 1179–1180.
[9] C. Lemoine, P. Besnier, and M. Drissi, "Investigation of reverberation chamber measurements through high-power goodness-of-fit tests," *IEEE Transactions on Electromagnetic Compatibility*, vol. 49, no. 4, pp. 745–755, 2007.
[10] G. Gradoni, F. Moglie, and V. M. Primiani, "Correlation matrix methods to assess the stirring performance of electromagnetic reverberation chambers," *Wave Motion*, vol. 87, pp. 213–226, 2019.
[11] G. Andrieu, N. Ticaud, and N. Roger, "On the number of independent samples available in a virc over a long exposition time and the potential detection of periodical stirring patterns," *IEEE Transactions on Electromagnetic Compatibility*, 2025.
[12] R. J. Pirkl, "Spatial autocovariances of scattering parameters measured in a lossy reverberation chamber," *IEEE transactions on electromagnetic compatibility*, vol. 55, no. 4, pp. 671–682, 2013.
[13] K. A. Remley, S. Catteau, A. Hussain, C. L. Nogueira, M. Kristoffersen, J. Kvarnstrand, B. Horrocks, J. Fridén, R. D. Horansky, and D. F. Williams, "Practical correlation-matrix approaches for standardized testing of wireless devices in reverberation chambers," *IEEE Open Journal of Antennas and Propagation*, vol. 4, pp. 408–426, 2023.
[14] J. Ali, L. Bastianelli, E. Colella, A. De Leo, F. Moglie, and V. M. Primiani, "Fdtd simulations of random boundaries," in *2025 International Symposium on Electromagnetic Compatibility–EMC Europe*. IEEE, 2025, pp. 1148–1152.
[15] R. J. Pirkl, K. A. Remley, and C. S. L. Patane, "Reverberation chamber measurement correlation," *IEEE Transactions on Electromagnetic Compatibility*, vol. 54, no. 3, pp. 533–545, 2012.
[16] D. A. Hill and J. M. Ladbury, "Spatial-correlation functions of fields and energy density in a reverberation chamber," *IEEE Transactions on Electromagnetic Compatibility*, vol. 44, no. 1, pp. 95–101, 2002.
[17] F. Moglie, L. Bastianelli, and V. M. Primiani, "Reliable finite-difference time-domain simulations of reverberation chambers by using equivalent volumetric losses," *IEEE Transactions on Electromagnetic Compatibility*, vol. 58, no. 3, pp. 653–660, 2016.